SEMARAK ILMU PUBLISHING

Journal of Advanced Research in Fluid Mechanics and Thermal Sciences

Journal homepage:
https://semarakilmu.com.my/journals/index.php/fluid_mechanics_thermal_sciences/index
ISSN: 2289-7879

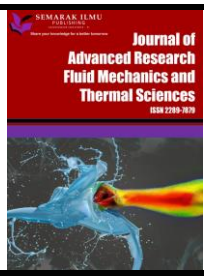

Analysis of GO-MoS_2/EG Powell-Eyring Fluid Transportation in Stagnation Point Flow and Heat Transfer over a Shrinking Surface

Nur Aisyah Aminuddin[1,2], Nor Ain Azeany Mohd Nasir[2,*], Norli Abdullah[3], Wasim Jamshed[4]

[1] Department of Defense Science, Faculty of Defense Science and Technology, National Defence University of Malaysia, Sungai Besi Camp, 57000 Kuala Lumpur, Malaysia
[2] Department of Mathematics, Centre for Defence Foundation Studies, National Defence University of Malaysia, Sungai Besi Camp, 57000 Kuala Lumpur, Malaysia
[3] Department of Chemistry and Biology, Centre for Defence Foundation Studies, National Defence University of Malaysia, Sungai Besi Camp, 57000 Kuala Lumpur, Malaysia
[4] Department of Mathematics, Capital University of Science and Technology (CUST), Islamabad, 44000, Pakistan

ARTICLE INFO

Article history:
Received 11 September 2023
Received in revised form 24 November 2023
Accepted 5 December 2023
Available online 31 December 2023

Keywords:
Non-Newtonian; hybrid nanofluid; entropy generation

ABSTRACT

Using ethylene glycol as the base fluid, nanomaterials graphene oxide (GO) and molybdenum disulfide (MoS_2) are disseminated into the fluid. The heat transfer behaviour of a non-Newtonian Powell-Eyring fluid hybrid nanofluid is evaluated together with several effects such as magnetic, suction and radiation. Ordinary differential equations (ODEs) are acquired by deriving the mathematical model in partial differential equations (PDEs) with suitable similarity transformations. The formulas are numerically estimated with the assistance of the bvp4c solver in MATLAB. The impact of parameter effects on the skin friction coefficient, local Nusselt number, entropy generation, velocity profile and temperature profile are reviewed and discussed. The aftermath revealed that skin friction and suction effects are elevated along the magnetic field. The rate of heat transmission is enhanced by improving the value of the suction parameter. Magnetic field, Eckert number and suction boosted entropy over the shrinking plate.

1. Introduction

Nanofluid is a type of fluid where a tiny particle measured in nanometers is submerged into a base fluid. Various nanoparticles can be used, usually metal oxides like graphene, alumina, molybdenum disulfide and copper. Nanofluid is a development used to improve the thermal properties of a conventional fluid because using only the base fluid provides low thermal conductivity. The idea of nanofluid was first introduced by Choi and Eastman [1]. A few years back, a new type of nanofluid was introduced to the industry. This fluid is created by combining two or more different types of nanoparticles and dispersing them into a base fluid. One of the gains of hybrid nanofluid is it can help reduce the cost since nanoparticles like copper, silver, and gold are expensive. Combining different particles requires only a tiny amount of each particle, hence why it is better than

* *Corresponding author.*
E-mail address: norainazeany@upnm.edu.my

https://doi.org/10.37934/arfmts.112.2.113

nanofluid. Moreover, much past research has proved that hybrid nanofluid can transmit heat more effectively than conventional nanofluid. Due to their relevant and good thermal conductivity, a lot of fields are utilizing both nanofluid and hybrid nanofluid, such as generators, thermal storage, coolant machines, medical devices, solar systems and welding. Hussain *et al.,* [2] looked into the flow of GO-MOS_2/H_2O subject to melting heat. For increasing volume fraction, the skin friction and Nusselt number are less in value for GO-MOS_2/H_2O compared to MOS_2/H_2O. Khan *et al.,* [3] explored the flow of GO-MOS_2/H_2O through slender revolution bodies. Due to the concentration of nanoparticles, the velocity of the fluid plunges for both nanofluid and hybrid nanofluid. Chu *et al.,* [4] inspected MHD GO-MOS_2/H_2O flow for a vertical cylinder with a shape factor. The temperature of the fluid was enlarged, and the velocity was depleted by the increment of magnetic parameters for both nanofluid and hybrid nanofluid. Khazayinejad and Nourazar [5] analyzed the flow of GO-Ag/H_2O considering an inclined magnetic field. The temperature of nanofluid Ag/H_2O can be improved by the insertion of GO, owing to the thermal conduction property of GO. Ramesh *et al.,* [6] examined the heat transfer of GO and aluminium alloy through a porous cylinder. The temperature of A7072-AA7075/H_2O is lower in comparison to the Fe_3O_4-GO /H_2O. Hussain and Jamshed [7] considered Cu-SiO_2/EG flow with the implementation of the finite difference method. The heat transfer rate of Cu-SiO2/EG is more efficient than Cu/EG. Mishra *et al.,* [8] evaluated the Non-Newtonian Casson Fluid Cu-Al_2O_3/EG flow. They concluded that adding the nanoparticles to the base fluid EG helps improve the fluid's thermophysical properties.

Magnetohydrodynamics (MHD) is an exploration of the behaviour of liquids that are conducted electrically, along with the presence of a magnetic field. The current that is produced by the magnetic field will pass by a moving fluid, which subsequently incites force in the fluid. The force is well recognized as the Lorentz force, which appears as a consequence of the MHD effect and is beneficial in the cooling process. Anuar *et al.,* [9] looked into Cu-Al_2O_3/H_2O MHD flow near the stagnation area in the presence of the homogeneous-heterogeneous condition. The magnetic parameter *M* is thinning the contracting sheet's momentum and thermal boundary layer. Using the Successive linearization method, Bhatti *et al.,* [10] evaluated the MHD stagnation point flow on a shrinking sheet. They deduced that the velocity of the fluid increases along with the magnetic parameter. Awaludin *et al.,* [11] studied stagnation point flow with heat sources and chemical reactions. They discovered that as the value of magnetic goes up, the solution is unique for elongating sheets, and for contracting plates, the solutions are not unusual. Sajjad *et al.,* [12] explored MHD Cu-Al_2O_3/H_2O on an upright contracting wedge with Joule heating and slip effects. They inferred that the magnetic field grows both the momentum and temperature of the liquid. Lund *et al.,* [13] inspected MHD 3D Cu-Al_2O_3/H_2O on a nonlinear shrinking plate using the 3-level Lobato Illa method and concluded that the magnetic effect diminishes both the velocity and temperature of the fluid. Another study by Lund *et al.,* [14] also proved that the magnetic field slows down the speed of the fluid. Their research included Stefan blowing and slip effects for MHD Casson nanofluid.

Non-Newtonian fluid has an inconstant viscosity. It relates to the shear stress, elasticity, and pressure changes. Most fluids used in real-life applications are considered non-Newtonian, such as dyes, lubricants, ketchup, chemical processing, paints, elastomers, and mining. The complicated behaviour of non-Newtonian fluid makes it difficult to analyse by using a basic equation or any Newtonian model. Hence, previous scholars created several non-Newtonian models to ease the study of shear stress and strain in the fluid. Some of the models for non-Newtonian are the power law, Casson, Maxwell, Jeffrey and Powell-Eyring models. The Powell-Eyring model was developed in 1944. Unlike other models, this model emerges directly from the dynamic of fluid theory, usually based on an empirical expression. Thus, even though the structure of this model is more complex, it is more beneficial. Prior studies that have utilized this model are the magnetically influenced Powell-

Eyring Cu-MeOH and GO-MeOH flow, Powell-Eyring Cu-Al_2O_3/H_2O and Cu/H_2O flow, MHD Powell-Eyring nano-liquid flow over a contracting wedge, Powell-Eyring fluid flow on a stretched plate, gyrotactic microorganisms in the Powell-Eyring fluid while considering radiation and suction effects, and C71500–Ti_6Al_4V/ $C_2H_6O_2$−H_2O fluid on a vertical plate with a heat source [15-20].

Entropy relates to the irreversibility level that takes place throughout a process. It tells the amount of disturbance produced, which dissipates the productivity of a system. The heat transmission process is founded on basic thermodynamic concepts. The first rule is related to energy conservation, and the second rule states that in a thermal process, the system's entropy must exist. Thermodynamically, the dysfunction is in the form of losing energy during the process as a consequence of several features and effects such as heat generation, radiation, suction, concentration level and many more. Entropy occurrence happens in ample real-life applications such as heating and cooling appliances, reactors, nuclear and solar technology, and sensors. That being the case, it is necessary to study how to control the production of disruption and preserve the energy in a system. Many scholars solved the problem of entropy generation in heat transfer, such as EMHD radiated Ag-TiO_2/Blood flow, EMHD Cu-Al_2O_3/H_2O flow near the stagnation point of an elongating plate with radiation, the influence of Lorentz force effect for Cu-Fe_3O_4/EG, mass-based GO-Fe_3O_4/H_2O flow for a convectively warmed stretching shrinking plate, CNTs-Cadmium telluride/EG flow with radiation and melting effects, impact of curvature on peristaltic thrusting of EMHD Cu-Al_2O_3/Blood, and flow of viscoelastic nanofluid over an elongating cylinder [21-27].

The first person that introduced the study of stagnation point flow was Hiemenz in the year 1911. The flow of the fluid near the stagnation point moves toward the plate orthogonally. Then, on a moving or stationary plate, the flow will be divided into two different directions. The velocity of the flow on the stagnation area is said to be zero or in a not-moving state. However, the pressure, heat transfer, mass deposition and heat transfer are at the highest value when they are close to the stagnation region. A few studies on stagnation point flow have been completed earlier, such as -CuO/H_2O flow when it was exposed to suction, EMHD Cu-Al_2O_3/H_2O flow on a vertical plate when it was revealed to slip and suction, SWCNTs-CuO/EG flow with melting heat, magnetic and heat source/sink effects, EMHD Cu-Al_2O_3/H_2O stagnation flow when velocity slip, viscous dissipation and radiation, Ag-CuO/H_2O stagnation flow on an exponentially contracting plate, and Casson nanofluid flow under the influence of Thompson and Troian slip [28-33]. Oblique stagnation flow also has been investigated, such as EMHD Cu-Al_2O_3/H_2O flow on a contracting surface and MWCNT-SWCNT/EG flow on an elongated cylinder [34,35].

As per the literature, only a few research have been dedicated to the flow of EG-based GO-MoS_2 hybrid nanofluid and the entropy analysis over a contracting plate. Motivated by the characteristics of non-Newtonian hybrid nanofluid and the importance of entropy analysis on a shrinking surface, this research covers those elements by analyzing the flow of GO-MoS_2/EG fluid on a porous plate with magnetic field, radiation, and suction effects. The usage of GO in this work is in line with the increasing utilization of GO in advanced applications. MoS_2 possesses an excellent catalytic feature and a favourable low value of friction. Suitable similarity transformations are used to convert partial differential equations into ordinary differential equations. The rapidity, temperature, skin friction coefficient, local Nusselt number and entropy generation are the main points that are being discussed and analyzed from figures and tables.

2. Mathematical Modelling

The flow of an incompressible Powell-Eyring hybrid nanofluid near a stagnation point along a porous horizontal flat plate is of interest, as indicated in Figure 1. The x and y are Cartesian

coordinates in which the x -axis is measured horizontally, and the y-axis is normal to the surface. The plane $y = 0$ corresponds with the flat plate, and the fluid flows inside $y \geq 0$. Horizontally, the plate extends and contracts where $u_w(x) = bx^{\frac{1}{3}}$, where $b > 0$ represents the stretching rate and $b < 0$ represents the shrinking rate. The ambient (inviscid) fluid velocity is $u_e(x) = ax^{\frac{1}{3}}$, where a is a positive constant. T_w is denoted as the surface temperature, while the far-field temperature of the hybrid nanofluid is known as T_∞. It is noteworthy when $T_w > T_\infty$ is an assisting flow and $T_w < T_\infty$ resembles the opposing flow. v_w is defined as the mass velocity, where the suction and injection parameters are noted as $v_w < 0$ and $v_w > 0$, respectively. The fluid parameters of the Powell-Eyring model are denoted by β^* and ε. B is the imposed magnetic field, where $B = B_0 x^{-\frac{1}{3}}$ and radiation heat flux is represented by q_r. Based on the above assumption, the governing boundary layer involved is modelled as follows [23,30,36]:

$$\frac{\partial u}{\partial x} + \frac{\partial v}{\partial y} = 0 \tag{1}$$

$$u\frac{\partial u}{\partial x} + v\frac{\partial u}{\partial y} = u_e\frac{\partial u_e}{\partial x} + \left(\nu_{hnf} + \frac{1}{\rho_{hnf}\beta^*\varepsilon}\right)\frac{\partial^2 u}{\partial y^2} - \frac{1}{2\rho_{hnf}\beta^*\varepsilon^3}\left(\frac{\partial u}{\partial y}\right)^2\frac{\partial^2 u}{\partial y^2} - \frac{\sigma_{hnf}B^2}{\rho_{hnf}}(u - u_e) \tag{2}$$

$$u\frac{\partial T}{\partial x} + v\frac{\partial T}{\partial y} = \frac{k_{hnf}}{(\rho C_p)_{hnf}}\left(\frac{\partial^2 T}{\partial y^2}\right) + \frac{\mu_{hnf}}{(\rho C_p)_{hnf}}\left(\frac{\partial u}{\partial y}\right)^2 - \frac{1}{(\rho C_p)_{hnf}}\left(\frac{\partial q_r}{\partial y}\right) \tag{3}$$

With boundary conditions of:

$$u = u_w(x) = bx^{\frac{1}{3}}, \quad v = v_w(x), \quad T = T_w(x) = T_\infty + T_0 x^{-\frac{1}{3}} \text{ at } y = 0$$

$$u \to u_e(x) = ax^{\frac{1}{3}}, \quad T \to T_\infty \text{ as } y \to \infty \tag{4}$$

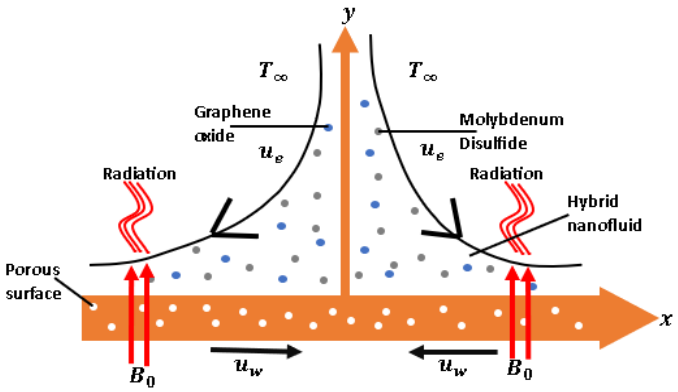

Fig. 1. Shrinking porous horizontal plate model

The appropriate similarity transformation is introduced as follows [36]:

$$\psi = \sqrt{\frac{3a\nu_f}{2}}x^{\frac{2}{3}}f(\eta), \quad \theta(\eta) = \frac{T - T_\infty}{T_w - T_\infty}, \quad \eta = y\sqrt{\frac{2a}{3\nu_f}}x^{-\frac{1}{3}} \tag{5}$$

It is widely known that the stream function is ψ where $u = \frac{\partial \psi}{\partial y}$ as well as $v = -\frac{\partial \psi}{\partial x}$. Then, u and v can be written as:

$$u = ax^{\frac{1}{3}}f', \quad v = -\frac{1}{3}\sqrt{\frac{3a\nu_f}{2}}x^{-\frac{1}{3}}S \tag{6}$$

It is noticeable that the differentiation concerning η is denoted as primes and the suction and injection parameters known as $S = 2f - \eta f'$ where $S > 0$ and $S < 0$ respectively. Using Eq. (5) and substituting into Eq. (1) to Eq. (4) will yield the reduced ordinary differential equations below:

$$\left(\frac{1}{\phi_a\phi_b} + \chi\frac{1}{\phi_b}\right)f''' - \frac{\chi\varsigma}{3\phi_b}f''^2f''' - \frac{1}{2}f'^2 + ff'' - \frac{3}{2}\frac{\phi_e}{\phi_b}M\,(f' - 1) + \frac{1}{2} = 0 \tag{7}$$

$$\frac{\phi_d}{Pr\phi_c}\left(1 + \frac{PrRd}{\phi_d}\right)\vartheta'' + \frac{Ec}{\phi_a\phi_c}f''^2 + f\vartheta' = 0 \tag{8}$$

Along with the boundary conditions:

$$f'(0) = \alpha,\ f(0) = S,\ \theta(0) = 1 \text{ at } \eta = 0$$

$$f'(\eta) \to 1, \quad \theta(\eta) \to 0 \text{ as } \eta \to \infty \tag{9}$$

where $\chi = \frac{1}{\mu_f\beta^*\boldsymbol{\varepsilon}}$ and $\varsigma = \frac{a^3}{\varepsilon^2\nu_f}$ are the material parameters, $M = \frac{\boldsymbol{\sigma_f}\,B_0^2}{a\boldsymbol{\rho_f}}$ is the magnetic field parameter, Pr is the Prandtl number, $Rd = \frac{16\sigma^*T_\infty^3}{\nu_f(\rho C_p)_f 3k^*}$ is radiation parameter, $Ec = \frac{u_e^2}{(T_w - T_\infty)(C_p)_f}$ is the Eckert number, S is suction and $\alpha = \frac{b}{a}$ is the stretching/shrinking parameter, where an elongating plate is denoted by $\alpha > 0$, and a contracting plate is depicted by $\alpha > 0$.

The hybrid nanofluid parameters are represented by [37]:

$$\phi_a = (1-\phi_1)^{2.5}(1-\phi_2)^{2.5} = \frac{\mu_f}{\mu_{hnf}} \tag{10}$$

$$\phi_b = (1-\phi_2)\left[(1-\phi_1) + \phi_1\frac{\rho_{s1}}{\rho_f}\right] + \phi_2\frac{\rho_{s2}}{\rho_f} = \frac{\rho_{hnf}}{\rho_f} \tag{11}$$

$$\phi_c = (1-\phi_2)\left[(1-\phi_1) + \phi_1\frac{(\rho C_p)_{s1}}{(\rho C_p)_f}\right] + \phi_2\frac{(\rho C_p)_{s2}}{(\rho C_p)_f} = \frac{(\rho C_p)_{hnf}}{(\rho C_p)_f} \tag{12}$$

$$\phi_d = \frac{k_{hnf}}{k_f}, \phi_e = \frac{\sigma_{hnf}}{\sigma_f} \tag{13}$$

The formulas used to calculate the values of hybrid nanofluid parameters $\phi_a, \phi_b, \phi_c, \phi_d, \phi_e$ based on their respective thermophysical characteristics can be found in Table 1. The thermo-physical properties for GO-MoS_2/EG hybrid nanofluid particles are recorded in Table 2. The provided values will be utilised for the computation of the hybrid nanofluid parameters $\phi_a, \phi_b, \phi_c, \phi_d, \phi_e$. The subscript $hnf, nf, f, s, s2$ is referred to as hybrid nanofluid, nanofluid, base fluid, first nanoparticle, and second nanoparticle, respectively.

Table 1
The features of thermo-physical hybrid nanofluids [38]

Features	Hybrid Nanofluid
Density (ρ)	$\rho_{hnf} = (1-\phi_2)\left[(1-\phi_1)\rho_f + \phi_1\rho_{s1}\right] + \phi_2\rho_{s2}$
Viscosity (μ)	$\mu_{hnf} = \mu_f/(1-\phi_1)^{2.5}(1-\phi_2)^{2.5}$
Heat capacity (ρC_p)	$(\rho C_p)_{hnf} = (1-\phi_2)\left[(1-\phi_1)(\rho C_p)_f + \phi_1(\rho C_p)_{s1}\right] + \phi_2(\rho C_p)_{s2}$
Thermal conductivity (k)	$k_{hnf} = \frac{k_{s2} + 2k_{nf} - 2\phi_2(k_{nf} - k_{s2})}{k_{s2} + 2k_{nf} + \phi_2(k_{nf} - k_{s2})} \times k_{nf}$
Electrical conductivity (σ)	$\sigma_{hnf} = \frac{\sigma_{s2} + 2\sigma_{nf} - 2\phi_2(\sigma_{nf} - \sigma_{s2})}{\sigma_{s2} + 2\sigma_{nf} + \phi_2(\sigma_{nf} - \sigma_{s2})} \times \sigma_{nf}$

Table 2
The values of nanoparticles and base fluid thermo-physical properties [39-41]

Thermophysical Properties	Graphene Oxide (GO)	Molybdenum Disulphide (MoS_2)	Ethylene Glycol (EG)
Thermal conductivity k	5000	34.5	0.253
Density ρ	1800	5060	1115
Specific heat C_p	717	397.746	2430
Electrical conductivity σ	$6.3\text{x}10^7$	$2.09\text{x}10^4$	$10.7\text{x}10^{-5}$

The relevant physical quantities are the skin-friction coefficient C_f, Nusselt number Nu_x and entropy generation N_G , where [36,37]:

$$C_f = \frac{\tau_w}{\rho_f u_e^2}, \qquad Nu_x = \frac{x q_w}{k_f(T_w - T_\infty)}, \qquad N_G = \frac{T_\infty^2 a^2 E_G}{k_f(T_w - T_\infty)^2} \tag{14}$$

Furthermore, shear stress is defined by $\tau_w = \left[\left(\mu_{hnf} + \frac{1}{\beta^*\varepsilon^3}\right)\frac{\partial u}{\partial y} - \frac{1}{4\beta^*\varepsilon^3}\left(\frac{\partial u}{\partial y}\right)^3\right]_{y=0}$, heat flux $q_w = -k_{hnf}\left[1 + \frac{16\sigma^* T_\infty^3}{3k^*\nu_f(\rho C_p)_f}\right]\left(\frac{\partial T}{\partial y}\right)_{y=0}$ and $E_G = \frac{k_{hnf}}{T_\infty^2}\left[\left(\frac{\partial T}{\partial y}\right)^2 + \frac{16\sigma^* T_\infty^3}{3k^*\nu_f(\rho C_p)_f}\left(\frac{\partial T}{\partial y}\right)^2\right] + \frac{\mu_{hnf}}{T_\infty}\left(\frac{\partial u}{\partial y}\right)^2$. By using the same transformations from (5) and (6), the physical quantities equations are reduced to:

$$C_f Re_x^{\frac{1}{2}} = \sqrt{\frac{3}{2}} Re_x^{1/2} C_f = \left(\frac{1}{\phi_a} + \chi\right) f''(0) - \frac{\chi\varsigma}{6} f'''(0), \qquad \sqrt{\frac{3}{2}} Re_x^{-1/2} Nu_x = -\phi_d\,(1+Rd)\vartheta'$$

$$\frac{3}{2} Re^{-1} N_G = \phi_d\,(1+Rd)\vartheta'^2 + \frac{B_r T_\infty}{\phi_a(T_w - T_\infty)}\, f''^2(0) \tag{15}$$

Some additional notations are the local Reynolds number $Re_x = \frac{x u_e}{\nu_f}$ and Brinkmann number $B_r = \frac{\mu_f u_e^2}{k_f(T_w - T_\infty)}$.

3. Discussion

The solver that is used in this work is the bvp4c solver built-in MATLAB due to its capability to manage PDEs that come with some complex boundary rules. For various values of the governing parameter , the fluid flow problem is analyzed numerically. With ethylene glycol EG as the base fluid,

the Prandtl number Pr is fixed as $\mathrm{Pr} = 204$ [42]. The concentration for both nanoparticles graphene oxide GO and molybdenum disulfide MoS_2 are 0.1. ϕ_1 and ϕ_2 indicate MoS_2 and GO, respectively.

The escalation of magnetic field M soars the skin friction as in Figure 2. As the speed of the fluid becomes faster, the skin friction in the system is also raised due to the creation of interference by Lorentz force within the boundary layer. Figure 3 shows that the intensification of M weakens the Nusselt number. The depleted Nusselt number depicts that the rate of heat transmission in the system is reduced. The production of entropy swells with the increment of M as in Figure 4. This relates a lot with the enhancement of temperature as M increases because this denotes that more energy is given to the particles, thus the amount of heat transmission out of the fluid contracts. Hence, the generation of interference, thermally, is boosted. A lot of friction is also generated because of the Lorentz force, which affects the amount of disturbance in the system. The critical value α_c gets smaller as M gets bigger, such that $\alpha_c = -2.5631$ ($M = 0.02$), $\alpha_c = -2.6304$ ($M = 0.05$) and $\alpha_c = -2.7438$ ($M = 0.1$). This phenomenon depicts that the magnetic field parameter weakens the separation of the boundary layer.

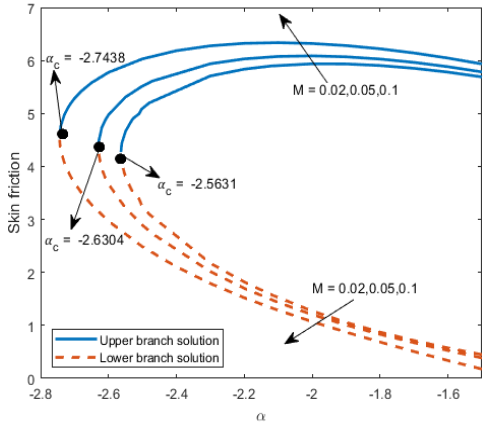

Fig. 2. $C_f Re_x^{\frac{1}{2}}$ for varied M and $\chi = 0.1$, $\varsigma = 0.1$, $Rd = 1.0$, $Ec = 0.1$, $S = 2$

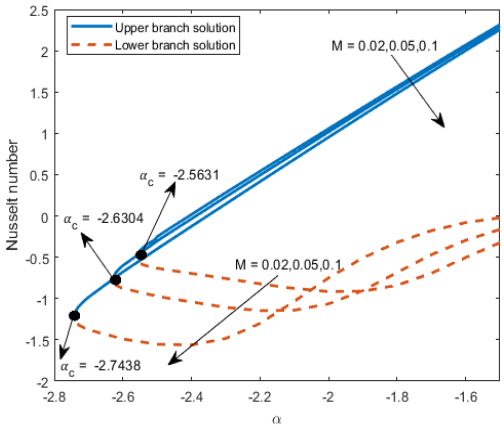

Fig. 3. $Nu_x Re_x^{-1/2}$ for varied M and $\chi = 0.1$, $\varsigma = 0.1$, $Rd = 1.0$, $Ec = 0.1$, $S = 2$

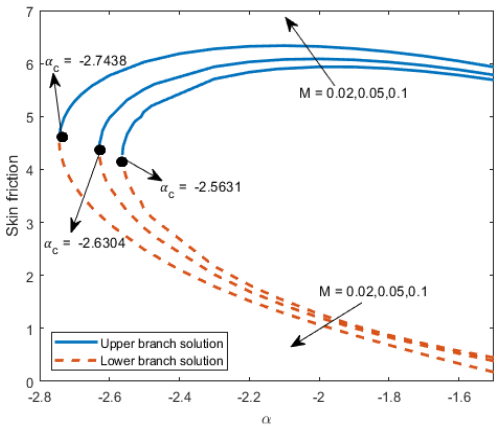

Fig. 4. $N_G . Re^{-1}$ for varied M and $\chi = 0.1$, $\varsigma = 0.1$, $Rd = 1.0$, $Ec = 0.1$, $S = 2$

Figure 5 displays that a higher concentration of graphene oxide ϕ_2 reduces the skin friction coefficient. Usually, the increment of volume fraction enhances skin friction because the collision among the particles is elevated, thus surging the skin friction of the system. However, based on Figure 5, it is illustrated that the skin friction diminished as ϕ_2 grows. The reason is the presence of holes

on the surface, and the suction effect attracts the flow, which leads to less flow near the plate, thus significantly affecting the decrement of skin friction. ϕ_2 slows down the local Nusselt number, as in Figure 6, which means that the system's heat transfer rate is diminishing as GO becomes more concentrated. The volume fraction's swelling elevates the liquid's temperature because more heat is absorbed into it. The enhancement of ϕ_2 diminishes the entropy generation, as in Figure 7. The increment of volume fraction apparently raises the count of collisions among the particles. Thus, the thermal energy inside the hybrid nanofluid is elevated due to the very compact condition. Hence, the generation of interference, thermally, is dwindled. The critical value α_c gets bigger as ϕ_2 rises, which dictates that ϕ_2 accelerates the boundary layer separation. Such that, $\alpha_c = -2.8117$ ($\phi_2 = 0.07$), $\alpha_c = -2.7438$ ($\phi_2 = 0.1$) and $\alpha_c = -2.7219$ ($\phi_2 = 0.11$).

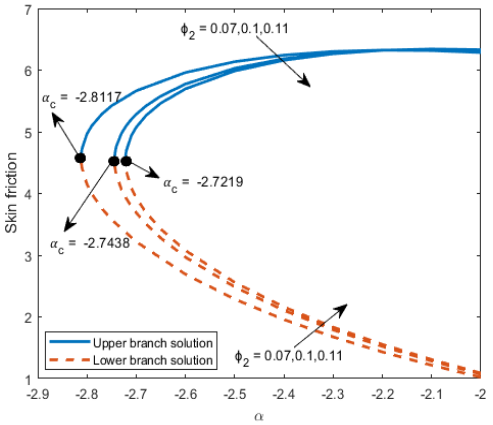

Fig. 5. $C_f Re_x^{\frac{1}{2}}$ for varied ϕ_2 *and* $\chi = 0.1$, $\varsigma = 0.1$, $M = 0.1$, $Rd = 1.0$, $Ec = 0.1$, $S = 2$

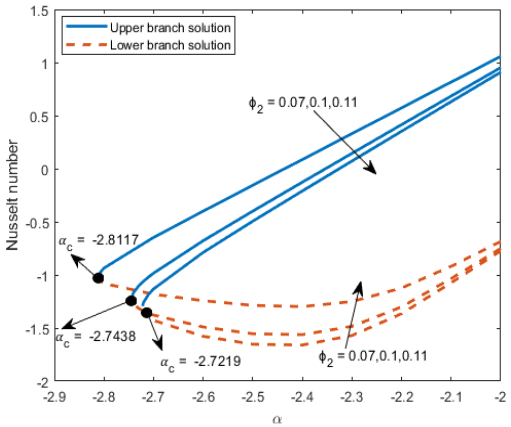

Fig. 6. $Nu_x Re_x^{-1/2}$ for varied ϕ_2 *and* $\chi = 0.1$, $\varsigma = 0.1$, $M = 0.1$, $Rd = 1.0$, $Ec = 0.1$, $S = 2$

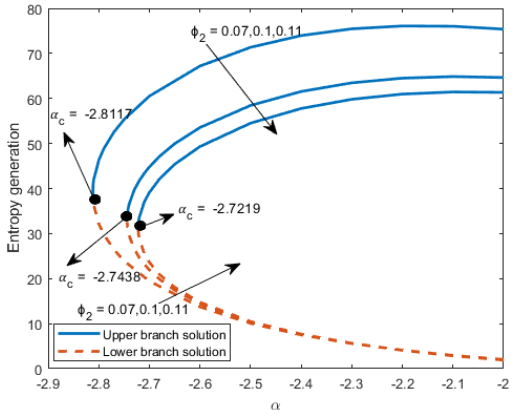

Fig. 7. $N_G . Re^{-1}$ for varied ϕ_2 *and* $\chi = 0.1$, $\varsigma = 0.1$, $M = 0.1$, $Rd = 1.0$, $Ec = 0.1$, $S = 2$

Figure 8 reveals that as the magnetic field M surges, the velocity of the fluid speeds up, and the momentum boundary layer becomes thinner. The existence of magnetic field somehow affects the augmentation of velocity. Moreover, the Lorentz force generated by the magnetic field does not restrain. Still, it pushes the flow, which is due to the linear relationship between the applied force with the magnetic field and the rapidity of the fluid. Figure 9 shows that as M escalates, the temperature of the fluid drops, and the thermal boundary layer gets narrower. More nanomaterials

are gathered on the wall due to the existence of Lorentz force, which makes the temperature of the plate become hotter instead of the fluid.

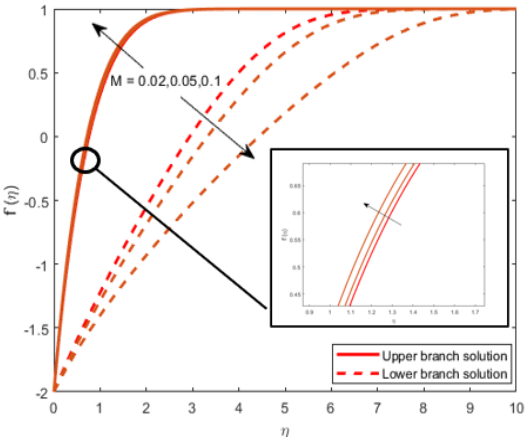

Fig. 8. $f'(\eta)$ for varied M *and* $\chi = 0.1$, $\varsigma = 0.1$, $Rd = 1.0$, $Ec = 0.1$, $S = 2$

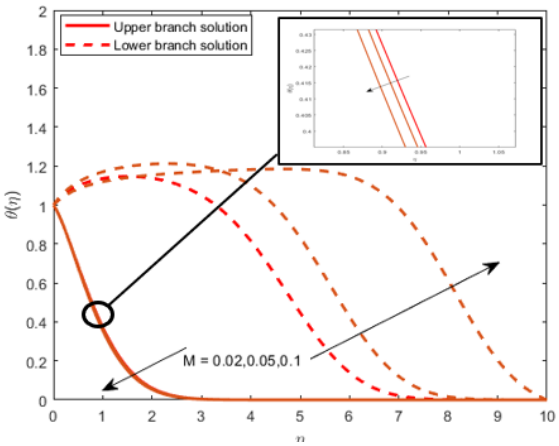

Fig. 9. $\vartheta(\eta)$ for varied M *and* $\chi = 0.1$, $\varsigma = 0.1$, $Rd = 1.0$, $Ec = 0.1$, $S = 2$

Figure 10 displays that the elevation of suction S boosts the velocity of the liquid and reduces the momentum boundary layer. Rationally, suction attracts more fluid to the slab, owing to the existence of holes on the plate. Hence, more drag force is produced near the plate due to the flow of hybrid nano liquid there. Figure 11 illustrates that the temperature of the fluid becomes colder, and the thermal boundary layer minimizes as the value of S hikes. The porous surface and high amount of suction lead to the cooling down of the temperature of the fluid, which leads to a higher heat transfer rate in the vicinity of the boundary layer.

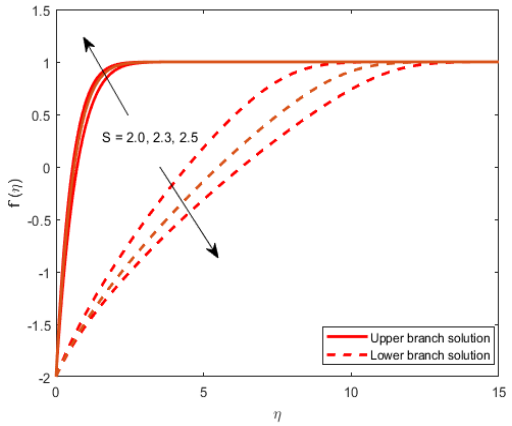

Fig. 10. $f'(\eta)$ for varied S *and* $\chi = 0.1$, $\varsigma = 0.1$, $M = 0.1$, $Rd = 1.0$, $Ec = 0.1$

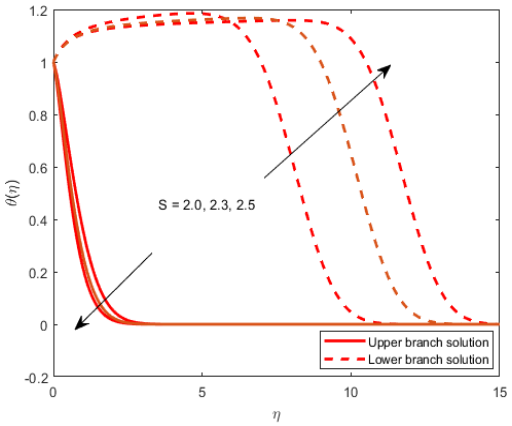

Fig. 11. $\vartheta(\eta)$ for varied S *and* $\chi = 0.1$, $\varsigma = 0.1$, $M = 0.1$, $Rd = 1.0$, $Ec = 0.1$

Figure 12 reveals that the concentration of graphene oxide ϕ_2 is elevated, the velocity of the liquid slows down. The viscosity of the fluid is enhanced, thus the magnification of the viscous force that leads to the drop of the velocity of the liquid. Figure 13 shows that the temperature of the fluid aggravates. Because of the high thermal conductivity of GO, more heat is transmitted into the fluid as ϕ_2 increases. The density of the fluid is also enhanced, which leads to the reduction of the space between the particles. For that reason, the molecules will bring out their thermal energy, and the rate of heat shifting is increased.

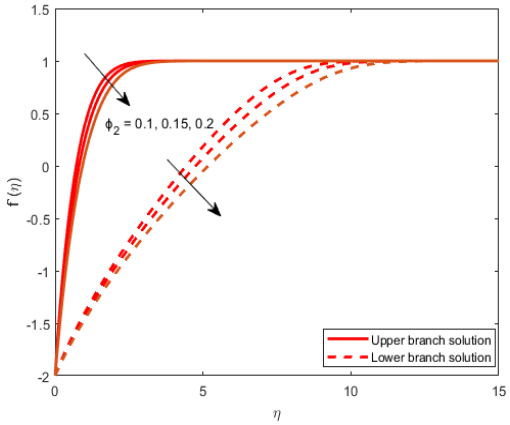

Fig. 12. $f'(\eta)$ for varied ϕ_2 *and* $\chi = 0.1$, $\varsigma = 0.1$, $M = 0.1$, $Rd = 1.0$, $Ec = 0.1$, $S = 2$

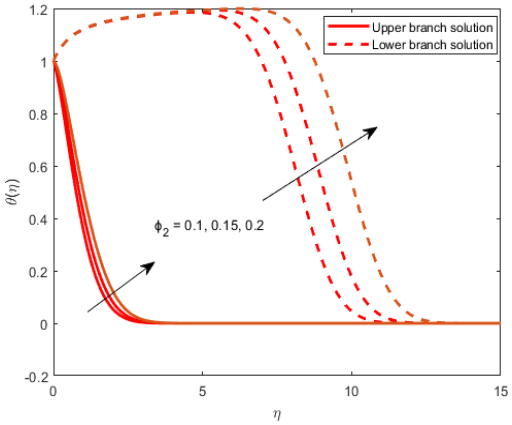

Fig. 13. $\vartheta(\eta)$ for varied ϕ_2 *and* $\chi = 0.1$, $\varsigma = 0.1$, $M = 0.1$, $Rd = 1.0$, $Ec = 0.1$, $S = 2$

Figure 14 displays that thermal radiation Rd inflates the temperature of the fluid and thickens the thermal boundary layer. With abundant radiation, more heat is transferred into the liquid since the bumping of molecules is enhanced, more energy conversion takes place in the flow, and higher heat flux is produced. Radiation has a direct relation with the internal energy of particles and temperature. Therefore, the temperature of the fluid will boost along with the value of radiation.

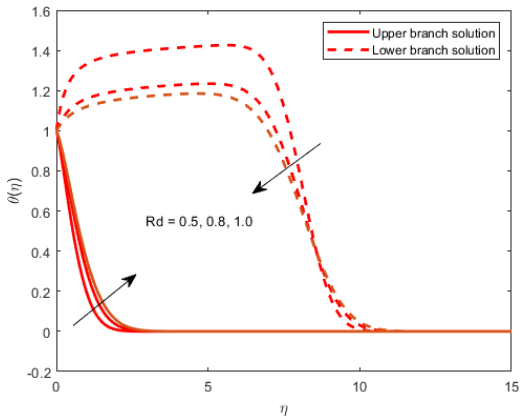

Fig. 14. $\vartheta(\eta)$ for varied Rd *and* $\chi = 0.1$, $\varsigma = 0.1$, $M = 0.1$, $Ec = 0.1$, $S = 2$

Figure 15 illustrates that Eckert number Ec swells the temperature of the liquid. When Ec is high, it denotes high kinetic energy. Higher Ec depletes the internal viscosity of hybrid nanofluid, then brings out tremendous internal energy in the flow where the kinetic energy turns into heat energy, hence adding up more heat to the fluid that ultimately enhances the temperature.

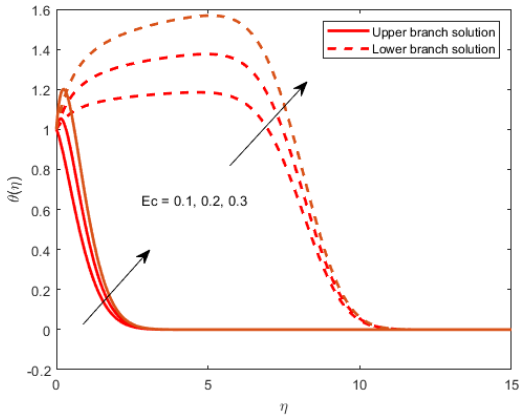

Fig. 15. $\vartheta(\eta)$ for varied Ec *and* $\chi = 0.1$, $\varsigma = 0.1$, $M = 0.1$, $Rd = 1.0$, $S = 2$

4. Conclusions

The analysis of non-Newtonian hybrid nanofluid GO-MOS_2/EG stagnation point flow on a contracting slab has been scrutinized with the influence of magnetic, radiation and suction. The results of this research paper are summarized as follows:

i. Magnetic and suction effects speed up the velocity of the fluid.
ii. The concentration of graphene oxide, radiation and Eckert number parameters elevate the temperature of the liquid.
iii. Magnetic field and suction boost the skin friction in the system.
iv. Suction promotes the rate of heat transmission in the system.
v. Magnetic field, Eckert number and suction encourage the generation of disturbance in the system.

Acknowledgement

This research was funded by a grant from Ministry of Higher Education of Malaysia and the National Defence University of Malaysia (FRGS Grant FRGS/1/2021/STG06/UPNM/02/1).

References

[1] Choi, S. U. S., and Jeffrey A. Eastman. *Enhancing thermal conductivity of fluids with nanoparticles*. No. ANL/MSD/CP-84938; CONF-951135-29. Argonne National Lab.(ANL), Argonne, IL (United States), 1995.

[2] Hussain, Zakir, Ali Saleh Alshomrani, Taseer Muhammad, and Muhammad Shoaib Anwar. "Entropy analysis in mixed convective flow of hybrid nanofluid subject to melting heat and chemical reactions." *Case Studies in Thermal Engineering* 34 (2022): 101972. https://doi.org/10.1016/j.csite.2022.101972

[3] Khan, Umair, Aurang Zaib, Mohsen Sheikholeslami, Abderrahim Wakif, and Dumitru Baleanu. "Mixed convective radiative flow through a slender revolution bodies containing molybdenum-disulfide graphene oxide along with generalized hybrid nanoparticles in porous media." *Crystals* 10, no. 9 (2020): 771. https://doi.org/10.3390/cryst10090771

[4] Chu, Yu-Ming, Kottakkaran Sooppy Nisar, Umair Khan, Hamed Daei Kasmaei, Manuel Malaver, Aurang Zaib, and Ilyas Khan. "Mixed convection in MHD water-based molybdenum disulfide-graphene oxide hybrid nanofluid through an upright cylinder with shape factor." *Water* 12, no. 6 (2020): 1723. https://doi.org/10.3390/w12061723

[5] Khazayinejad, Mehdi, and S. S. Nourazar. "Space-fractional heat transfer analysis of hybrid nanofluid along a permeable plate considering inclined magnetic field." *Scientific Reports* 12, no. 1 (2022): 5220. https://doi.org/10.1038/s41598-022-09179-9

[6] Ramesh, G. K., S. A. Shehzad, A. Rauf, and A. J. Chamkha. "Heat transport analysis of aluminum alloy and magnetite graphene oxide through permeable cylinder with heat source/sink." *Physica Scripta* 95, no. 9 (2020): 095203. https://doi.org/10.1088/1402-4896/aba5af

[7] Hussain, Syed M., and Wasim Jamshed. "A comparative entropy based analysis of tangent hyperbolic hybrid nanofluid flow: Implementing finite difference method." *International Communications in Heat and Mass Transfer* 129 (2021): 105671. https://doi.org/10.1016/j.icheatmasstransfer.2021.105671

[8] Mishra, S. R., P. Mathur, and P. K. Pattnaik. "Hybrid nanofluid flow of non-Newtonian Casson fluid for the analysis of Entropy through a permeable medium." *Journal of Nanofluids* 11, no. 3 (2022): 328-339. https://doi.org/10.1166/jon.2022.1846

[9] Anuar, Nur Syazana, Norfifah Bachok, and Ioan Pop. "Cu-Al_2O_3/water hybrid nanofluid stagnation point flow past MHD stretching/shrinking sheet in presence of homogeneous-heterogeneous and convective boundary conditions." *Mathematics* 8, no. 8 (2020): 1237. https://doi.org/10.3390/math8081237

[10] Bhatti, Muhammad Mubashir, M. Ali Abbas, and Mohammad Mehdi Rashidi. "A robust numerical method for solving stagnation point flow over a permeable shrinking sheet under the influence of MHD." *Applied Mathematics and Computation* 316 (2018): 381-389. https://doi.org/10.1016/j.amc.2017.08.032

[11] Awaludin, Izyan Syazana, Anuar Ishak, and Ioan Pop. "Stagnation Point Flow Over a Permeable Stretching/Shrinking Sheet with Chemical Reaction and Heat Source/Sink." *CMES-Computer Modeling in Engineering & Sciences* 120, no. 1 (2019). https://doi.org/10.32604/cmes.2019.06594

[12] Sajjad, Muhammad, Ali Mujtaba, Adnan Asghar, and Teh Yuan Ying. "Dual solutions of magnetohydrodynamics Al_2O_3+ Cu hybrid nanofluid over a vertical exponentially shrinking sheet by presences of joule heating and thermal slip condition." *CFD Letters* 14, no. 8 (2022): 100-115. https://doi.org/10.37934/cfdl.14.8.100115

[13] Lund, Liaquat Ali, Zurni Omar, Ilyas Khan, and El-Sayed M. Sherif. "Dual branches of MHD three-dimensional rotating flow of hybrid nanofluid on nonlinear shrinking sheet." *Computers, Materials and Continua* 66, no. 1 (2020): 127-139. https://doi.org/10.32604/cmc.2020.013120

[14] Lund, Liaquat Ali, Zurni Omar, Jawad Raza, Ilyas Khan, and El-Sayed M. Sherif. "Effects of Stefan blowing and slip conditions on unsteady MHD Casson nanofluid flow over an unsteady shrinking sheet: dual solutions." *Symmetry* 12, no. 3 (2020): 487. https://doi.org/10.3390/sym12030487

[15] Jamshed, Wasim, Mohamed R. Eid, Kottakkaran Sooppy Nisar, Nor Ain Azeany Mohd Nasir, Abhilash Edacherian, C. Ahamed Saleel, and V. Vijayakumar. "A numerical frame work of magnetically driven Powell-Eyring nanofluid using single phase model." *Scientific Reports* 11, no. 1 (2021): 16500. https://doi.org/10.1038/s41598-021-96040-0

[16] Aziz, Asim, Wasim Jamshed, Taha Aziz, Haitham M. S. Bahaidarah, and Khalil Ur Rehman. "Entropy analysis of Powell-Eyring hybrid nanofluid including effect of linear thermal radiation and viscous dissipation." *Journal of Thermal Analysis and Calorimetry* 143 (2021): 1331-1343. https://doi.org/10.1007/s10973-020-10210-2

[17] Raju, C. H., C. Srinivas Reddy, Maryam Ahmed Alyami, Sayed M. Eldin, Kanayo Kenneth Asogwa, D. Pushpa, and V. Dharmaiah. "MHD Eyring-Powell nanofluid flow across a wedge with convective and thermal radiation." *Frontiers in Energy Research* (2022): 1565. https://doi.org/10.3389/fenrg.2022.1021491

[18] Lawal, Matthew O., Kazeem B. Kasali, Hammed A. Ogunseye, Michael O. Oni, Yusuf O. Tijani, and Yussuff T. Lawal. "On the mathematical model of Eyring-Powell nanofluid flow with non-linear radiation, variable thermal conductivity and viscosity." *Partial Differential Equations in Applied Mathematics* 5 (2022): 100318. https://doi.org/10.1016/j.padiff.2022.100318

[19] Khan, Naseer M., Awatef Abidi, Ilyas Khan, Fakhirah Alotaibi, Abdulaziz H. Alghtani, M. A. Aljohani, and Ahmed M. Galal. "Dynamics of radiative Eyring-Powell MHD nanofluid containing gyrotactic microorganisms exposed to surface suction and viscosity variation." *Case Studies in Thermal Engineering* 28 (2021): 101659. https://doi.org/10.1016/j.csite.2021.101659

[20] Roja, A. "Scrutinization of entropy on MHD Eyring-Powell C71500-Ti_6Al_4V nanoparticles suspended in a $C_2H_6O_2$–H_2O hybrid base fluid with heat generation." *Heat Transfer* 51, no. 1 (2022): 193-209. https://doi.org/10.1002/htj.22302

[21] Saleem, Najma, Sufian Munawar, and Dharmendra Tripathi. "Entropy analysis in ciliary transport of radiated hybrid nanofluid in presence of electromagnetohydrodynamics and activation energy." *Case Studies in Thermal Engineering* 28 (2021): 101665. https://doi.org/10.1016/j.csite.2021.101665

[22] Kayalvizhi, J., and A. G. Vijaya Kumar. "Entropy Analysis of EMHD Hybrid Nanofluid Stagnation Point Flow over a Porous Stretching Sheet with Melting Heat Transfer in the Presence of Thermal Radiation." *Energies* 15, no. 21 (2022): 8317. https://doi.org/10.3390/en15218317

[23] Unyong, B., R. Vadivel, M. Govindaraju, R. Anbuvithya, and Nallappan Gunasekaran. "Entropy analysis for ethylene glycol hybrid nanofluid flow with elastic deformation, radiation, non-uniform heat generation/absorption, and inclined Lorentz force effects." *Case Studies in Thermal Engineering* 30 (2022): 101639. https://doi.org/10.1016/j.csite.2021.101639

[24] Berrehal, Hamza, Saeed Dinarvand, and Ilyas Khan. "Mass-based hybrid nanofluid model for entropy generation analysis of flow upon a convectively-warmed moving wedge." *Chinese Journal of Physics* 77 (2022): 2603-2616. https://doi.org/10.1016/j.cjph.2022.04.017

[25] Naqvi, Syed Muhammad Raza Shah, Hassan Waqas, Sumeira Yasmin, Dong Liu, Taseer Muhammad, Sayed M. Eldin, and Shan Ali Khan. "Numerical simulations of hybrid nanofluid flow with thermal radiation and entropy generation effects." *Case Studies in Thermal Engineering* 40 (2022): 102479. https://doi.org/10.1016/j.csite.2022.102479

[26] Mekheimer, Khaled S., Rabea E. Abo-Elkhair, Khalid K. Ali, and Moustafa G. Keshta. "Entropy generation and curvature effect on peristaltic thrusting of (Cu-Al_2O_3) hybrid nanofluid in resilient channel: Nonlinear analysis." *Heat Transfer* 50, no. 8 (2021): 7918-7948. https://doi.org/10.1002/htj.22260

[27] Usman, Auwalu Hamisu, Sadiya Ali Rano, Usa Wannasingha Humphries, and Poom Kumam. "Activity of viscoelastic nanofluid film sprayed on a stretching cylinder with Arrhenius activation energy and entropy generation." *Journal of Advanced Research in Micro and Nano Engineering* 3, no. 1 (2021): 12-24.

[28] Arani, Ali Akbar Abbasian, and Hossein Aberoumand. "Stagnation-point flow of Ag-CuO/water hybrid nanofluids over a permeable stretching/shrinking sheet with temporal stability analysis." *Powder Technology* 380 (2021): 152-163. https://doi.org/10.1016/j.powtec.2020.11.043

[29] Zangooee, M. R., Kh Hosseinzadeh, and D. D. Ganji. "Hydrothermal analysis of hybrid nanofluid flow on a vertical plate by considering slip condition." *Theoretical and Applied Mechanics Letters* 12, no. 5 (2022): 100357. https://doi.org/10.1016/j.taml.2022.100357

[30] Al Nuwairan, Muneerah, Abdul Hafeez, Asma Khalid, and Anwar Aldhafeeri. "Multiple solutions of melting heat transfer of MHD hybrid based nanofluid flow influenced by heat generation/absorption." *Case Studies in Thermal Engineering* 35 (2022): 101988. https://doi.org/10.1016/j.csite.2022.101988

[31] Nandi, Susmay, Bidyasagar Kumbhakar, and Gauri Shanker Seth. "Quadratic regression analysis of unsteady MHD free convective and radiative-dissipative stagnation flow of hybrid nanofluid over an exponentially stretching surface under porous medium." *Chinese Journal of Physics* 77 (2022): 2090-2105. https://doi.org/10.1016/j.cjph.2021.12.011

[32] Anuar, Nur Syazana, Norfifah Bachok, Norihan Md Arifin, and Haliza Rosali. "Effect of suction/injection on stagnation point flow of hybrid nanofluid over an exponentially shrinking sheet with stability analysis." *CFD Letters* 11, no. 12 (2019): 21-33.

[33] Akaje, Wasiu, and B. I. Olajuwon. "Impacts of Nonlinear thermal radiation on a stagnation point of an aligned MHD Casson nanofluid flow with Thompson and Troian slip boundary condition." *Journal of Advanced Research in Experimental Fluid Mechanics and Heat Transfer* 6, no. 1 (2021): 1-15.

[34] Yahaya, Rusya Iryanti, Norihan Md Arifin, Roslinda Mohd Nazar, and Ioan Pop. "Oblique Stagnation-Point Flow Past a Shrinking Surface in a Cu-Al." *Sains Malaysiana* 50, no. 10 (2021): 3139-3152. https://doi.org/10.17576/jsm-2021-5010-25

[35] Chu, Yu-Ming, M. Ijaz Khan, Tasawar Abbas, Maawiya Ould Sidi, Khalid Abdulkhaliq M. Alharbi, Umar F. Alqsair, Sami Ullah Khan, M. Riaz Khan, and M. Y. Malik. "Radiative thermal analysis for four types of hybrid nanoparticles subject to non-uniform heat source: Keller box numerical approach." *Case Studies in Thermal Engineering* 40 (2022): 102474. https://doi.org/10.1016/j.csite.2022.102474

[36] Naganthran, Kohilavani, Roslinda Nazar, and Ioan Pop. "A study on non-Newtonian transport phenomena in a mixed convection stagnation point flow with numerical simulation and stability analysis." *The European Physical Journal Plus* 134 (2019): 1-14. https://doi.org/10.1140/epjp/i2019-12454-0

[37] Qureshi, Muhammad Amer. "A case study of MHD driven Prandtl-Eyring hybrid nanofluid flow over a stretching sheet with thermal jump conditions." *Case Studies in Thermal Engineering* 28 (2021): 101581. https://doi.org/10.1016/j.csite.2021.101581

[38] Devi, S. P. Anjali, and S. Suriya Uma Devi. "Numerical investigation of hydromagnetic hybrid Cu-Al_2O_3/water nanofluid flow over a permeable stretching sheet with suction." *International Journal of Nonlinear Sciences and Numerical Simulation* 17, no. 5 (2016): 249-257. https://doi.org/10.1515/ijnsns-2016-0037

[39] Alwawi, Firas A., Hamzeh T. Alkasasbeh, A. M. Rashad, and Ruwaidiah Idris. "Heat transfer analysis of ethylene glycol-based Casson nanofluid around a horizontal circular cylinder with MHD effect." *Proceedings of the Institution of Mechanical Engineers, Part C: Journal of Mechanical Engineering Science* 234, no. 13 (2020): 2569-2580. https://doi.org/10.1177/0954406220908624

[40] Bagh, Ali, Rizwan Ali Naqvi, Dildar Hussain, Omar M. Aldossary, and Sajjad Hussain. "Magnetic Rotating Flow of a Hybrid Nano-Materials Ag-MoS_2 and Go-MoS_2 in $C_2H_6O_2$-H_2O Hybrid Base Fluid over an Extending Surface Involving Activation Energy: FE Simulation." *Mathematics* 8, no. 10 (2020): 1730. https://doi.org/10.3390/math8101730

[41] Yaseen, Moh, Sawan Kumar Rawat, Anum Shafiq, Manoj Kumar, and Kamsing Nonlaopon. "Analysis of heat transfer of mono and hybrid nanofluid flow between two parallel plates in a Darcy porous medium with thermal radiation and heat generation/absorption." *Symmetry* 14, no. 9 (2022): 1943. https://doi.org/10.3390/sym14091943

[42] Ganesh, N. Vishnu, Qasem M. Al-Mdallal, and P. K. Kameswaran. "Numerical study of MHD effective Prandtl number boundary layer flow of γ Al_2O_3 nanofluids past a melting surface." *Case Studies in Thermal Engineering* 13 (2019): 100413. https://doi.org/10.1016/j.csite.2019.100413